# Load Rating of Bridge LOG-47-1184

# Division of Engineering ROC Task 5

Prepared by Issam Khoury, Eric Steinberg, and Ahmadudin Burhani

Prepared for the Ohio Department of Transportation
Office of Statewide Planning and Research

State Job Number 135785

October 2019

*Final Technical Report*

**Ohio Research Institute for Transportation and the Environment**

| | | |
|---|---|---|
| **1. Report No.**<br>FHWA/OH-2019/24 | **2. Government Accession No.** | **3. Recipient's Catalog No.** |
| **4. Title and Subtitle**<br>Load Rating of Bridge LOG-47-1184<br>Engineering Research Services 2017-2020 Task 5 | | **5. Report Date**<br>October 2019 |
| | | **6. Performing Organization Code** |
| **7. Author(s)**<br>Issam Khoury, Eric Steinberg, and Ahmadudin Burhani | | **8. Performing Organization Report No.** |
| **9. Performing Organization Name and Address**<br>Ohio Research Institute for Transportation and the Environment (ORITE)<br>233 Stocker Center<br>Ohio University<br>Athens OH 45701-2979 | | **10. Work Unit No. (TRAIS)** |
| | | **11. Contract or Grant No.**<br>State Job No. 135785 |
| **12. Sponsoring Agency Name and Address**<br>Ohio Department of Transportation<br>Office of Research and Development<br>1980 West Broad St.<br>Columbus OH 43223 | | **13. Type of Report and Period Covered**<br>Final Technical Report |
| | | **14. Sponsoring Agency Code** |

**15. Supplementary Notes**

Prepared in cooperation with the Ohio Department of Transportation (ODOT) and the U.S. Department of Transportation, Federal Highway Administration

**16. Abstract**

Bridge LOG-47-1184, a four-lane concrete highway bridge, was instrumented and subjected to controlled vehicle load testing in May 2019. The load response data collected were used to generate load Rating Factors (RFs) via a three-dimensional finite element model (FEM) created using ABAQUS, which were compared to those generated by MIDAS/Civil software, and those from the original BrR analysis by the Ohio Department of Transportation (ODOT) following the AASHTO method. The RFs from the FEM were higher than those from MIDAS/Civil which were higher than those from the original BrR method. The ratios of the BrR RFs to the other methods were generally constant over several test truck load configurations, with less than 4% variation for BrR/MIDAS and about 25% for BrR/ABAQUS. This suggests that considerably higher RFs can be used than those generated by the conservative BrR method, however these conclusions apply to this specific bridge and the corresponding ratios determined for other concrete slab bridges may differ.

| | |
|---|---|
| **17. Key Words**<br>Bridge, load rating factors, finite element analysis. | **18. Distribution Statement**<br>No Restrictions. This document is available to the public through the National Technical Information Service, Springfield, Virginia 22161 |

| | | | |
|---|---|---|---|
| **19. Security Classif. (of this report)**<br>Unclassified | **20. Security Classif. (of this page)**<br>Unclassified | **21. No. of Pages**<br>24 | **22. Price** |

# Load Rating of Bridge LOG-47-1184

# Division of Engineering ROC
# Task 5

Prepared by

Issam Khoury, Eric Steinberg, and Ahmadudin Burhani

Ohio Research Institute for Transportation and the Environment
Russ College of Engineering and Technology
Ohio University
Athens, Ohio 45701-2979

Prepared in cooperation with the
Ohio Department of Transportation
and the
U.S. Department of Transportation, Federal Highway Administration



Final Technical Report
September 2019

## Acknowledgments

The authors would like to thank ODOT for their support of this project. The Technical Advisory Committee for the project included Jeremy Fisher, Tim Keller, and Amjad Waheed, all from the Office of Structural Engineering. Michelle Lucas handled project administration details at Central Headquarters.

We also thank Matt Blythe, head of the Structures Engineering Squad in the District 7 Design group, and Tim Little, Transportation Administrator of the Logan County Garage.

Graduate student Caden Brooker assisted with the field work, as did ORITE Operations Manager Joshua Jordan.

# Contents

## List of Figures



## List of Tables

## Project Background

LOG-47-1184 is a variable-depth three-span concrete slab bridge on State Route 47 in the city of Bellefontaine in Logan County, Ohio built in 1970 over CSX (formerly Penn Central) railroad tracks (see Figure 1). This bridge had previously been load rated by ODOT using PC BARS software, which analyzed the bridge at the locations of the maximum positive and negative moments. ODOT is required by the FHWA to determine load ratings for all their bridges for additional truck configurations. ODOT now utilizes the AASHTO BrR software to do the analysis for these new truck configurations as PC BARS is no longer supported. The BrR software evaluates more locations on the bridge. The BrR load rating indicated that the bridge should be load posted because the reinforcing steel in the negative moment region does not extend far enough. This controlling location on the bridge had not been evaluated in the previous load rating by the PC BARS. LOG-47-1184 has had permit vehicles routed over this structure in the past and shown no sign of distress. ODOT believes that the bridge has more capacity than the BrR analysis indicates. Verifying this bridge has more capacity than our current analytical tools indicate and calibrating the results will allow ODOT to use this procedure on similar structures statewide.

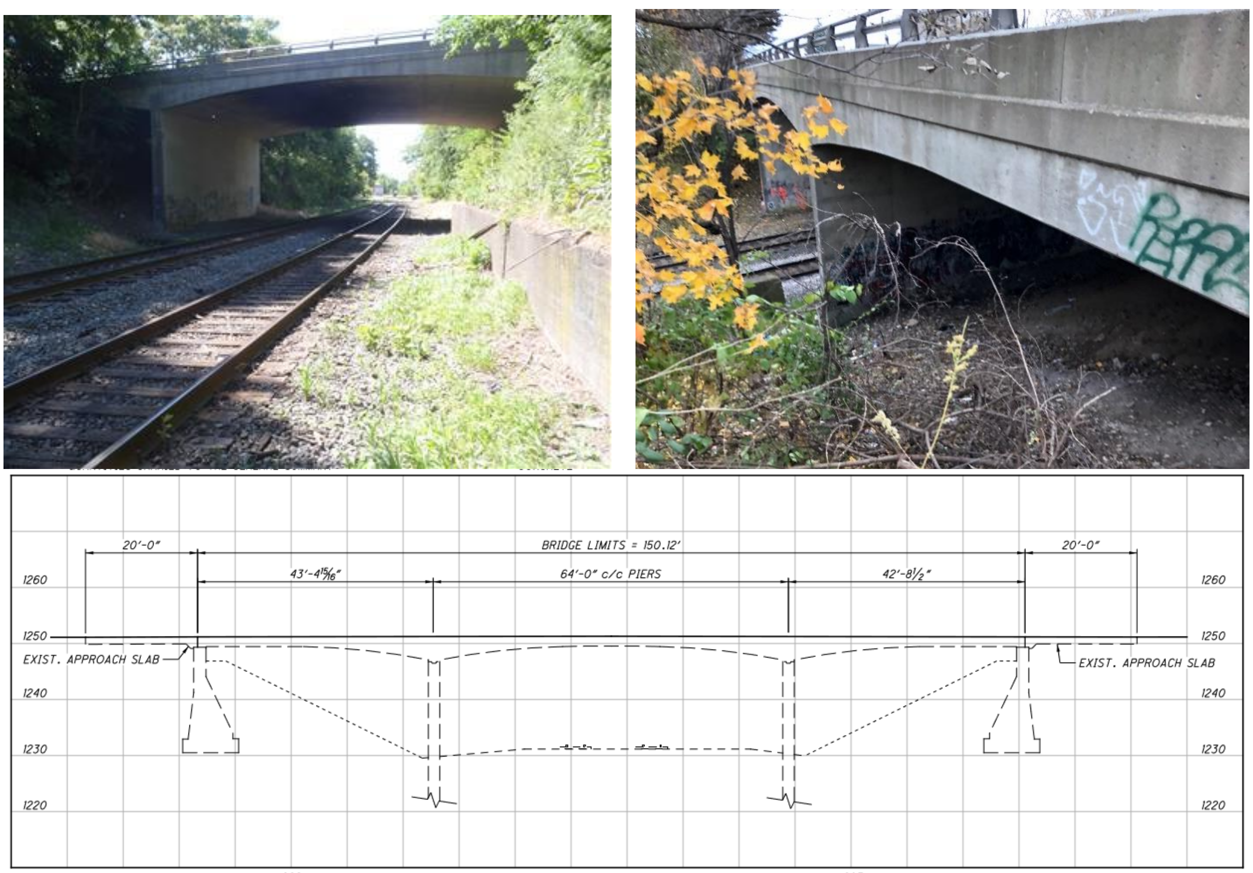


**Figure 1. Views of Bridge LOG-47-1184. Photographs of span (top) and profile drawing (bottom) (1' = 0.305 m; 1" = 0.0254 m)**

LOG-47-1184 is a variable-depth three-span concrete slab bridge. Span 1 from the west abutment is just slightly less than 43 ft 5 in (13.2 m) in length. Span 2 over the railroad is 64 ft (19.5 m) long, and Span 3 is 42 ft 8.5 in (13.0 m) long. The bridge has a 14°29′ right forward skew. The reinforced concrete deck is 4 ft 1.75 in (1.26 m) thick at the face of the piers and 1 ft 8.5 in (0.52 m) thick at the centerline of the mid-spans. According to plans, top longitudinal reinforcement over the piers consists of No. 11 (1.41 in or 35.8 mm diameter) bars spaced 6.5 in (165 mm) with No. 5 (0.625 in or 15.9 mm diameter) bars spaced at 13 in (330 mm) away from the piers toward the mid-spans. The No. 11 bars extend 18 ft (5.5 m) from the centerline of the piers in each direction.

## Objective

The objective of the project was to compute the Load Rating Factors of Bridge LOG-47-1184 and compare to prior results generated by ODOT. The expectation is that BrR under-reports the load the bridge can handle. By providing a calibrated and validated analytical tool that computes a more accurate load rating, it was anticipated that ODOT can use this procedure on similar structures statewide.

## Method

In order to evaluate the bridge's load rating more accurately, the following steps were taken by the research team:

- Literature was reviewed to obtain information related to the research. In addition, documentation provided by ODOT related to LOG-47-1184 bridge and its load rating was analyzed.
- Structural analyses of the bridge were performed using FEM models to determine critical locations subject to maximum moments in order to plan the placement of instrumentation.
- LOG-47-1184 was instrumented according to the plan developed using the critical locations determined in the structural analyses.
- Controlled vehicle load tests were performed on LOG-47-1184 to determine strains and deflections at the instrumented locations on the bridge. One lane was shut down to allow for instrumentation and loading by a truck with known wheel loads. Both static and moving load tests were conducted.
- Using the data obtained from the load testing, more advanced 3-D FEM models were calibrated to reduce assumptions in the initial modeling. These models were used to determine the load rating and compare to earlier load ratings made by ODOT.

## Literature Review

Saraf [1998] conducted load tests on three continuous reinforced concrete slab bridges which had minor to severe deterioration. An instrumentation plan was prepared and for a single span of each bridge based on the location of the most severe deterioration. Then a loaded truck was placed on each bridge at the position creating the maximum moments and shears. The field measurement results were compared and closely matched to those from calibrated finite element models (FEMs). The calibrated finite element models were used to compute new rating factors for all tested structures. The rating factors were also calculated using the procedure presented for reinforced concrete slab bridges in the AASHTO *Manual for condition evaluation of bridges* [AASHTO, 1994] and the equivalent strip width method described in the AASHTO Standard

*Specifications for highway bridges* [AASHTO, 1992]. The AASHTO rating approach was found to be overly conservative compared to the FEM method. It was mentioned that the equivalent strip width method overestimated the loading effects. The finite element model predicted an increase of 110% in the safe rating factor.

Davids et al. [2013] developed finite element software to determine the load rating of existing concrete slab bridges. These ratings were compared with those from the AASHTO equivalent strip width procedure for several slab bridges. The results were further used to verify accuracy of the developed software (called Slab Rate) as well as to validate experimental data under actual loading configurations. The authors concluded that finite element analysis could be an appropriate tool to conservatively predict concrete slab bridge response compared to the results obtained from load tests data. Even so, the finite element analyses predicted significantly higher results than the AASHTO equivalent strip width procedure. On average, there was approximately a 26% increase in the rating factors predicted by the FEM for several of the short-span bridges. Similarly, there was an average increase in rating factors of 27.3% for slab bridges with skew angles of 10.25º or less, and a 37.6% increase for structures with skew angles of 15º to 20º. It was concluded that the increase in the FEM rating factors grew with the skew angle. The authors implied that numerous slab bridges which are at risk of load posting based on the AASHTO equivalent strip method might actually have enough structural capacity, or those bridges with apparent structural deficiencies may not require (as much) strengthening.

Miller et al. [1992] evaluated the responses of a single-lane three-span skewed reinforced concrete slab bridge. The bridge was instrumented, and nondestructive tests such as truck testing were performed before the bridge was actually destroyed. The instrumentation measured the deflections under truck loads and determined the vibrational mode shape of the bridge. Up to three loaded dump trucks were placed on the bridge and the data were recorded. The recorded deflections and calculated vibrational mode shapes were compared with those from finite element models, and agreement was good between measured and predicted deflections for undamaged areas. Hidden deterioration and damage under the asphalt layer near the shoulders was reported. In this area, the finite element models underestimated the measured deflection by 20%. Upon completion of nondestructive tests, the bridge was loaded to failure. The failure occurred in flexural shear at a total load of 720,000 lb (3203 kN). Although the bridge had a factor of safety of about 7 against failure, none of the models could predict the shear failure appropriately. The author concluded that deteriorated or decommissioned reinforced concrete slab bridges may sustain a load several times larger than that predicted from current analysis techniques.

## Initial Structural Analyses to Determine Critical Sections

A preliminary analysis was conducted based on the information in the original design plans provided by the ODOT and an initial visual inspection. MIDAS/Civil numerical software was employed, and a full 3-D FEM of the slab bridge created using the dimensions from the structural drawings. The connections between abutments and the deck were modeled with pins. The piers were fixed at the bottom. Linear elastic links were used to connect the piers to the variable slabs. In the model, the westbound driving lane of the bridge was loaded with an Ohio 3F1 legal load tandem axle truck to determine the load position which would produce the highest moments. The maximum negative moment was found when the truck was positioned at 978 in (81.5 ft or 24.84 m, all dimensions are entered into MIDAS/Civil in inches) away from the right (east) abutment. The MIDAS/Civil output showing the truck position and resulting moment distribution is given in Figure 2 and a bridge profile showing the geometric details of the load is given in Figure 3.

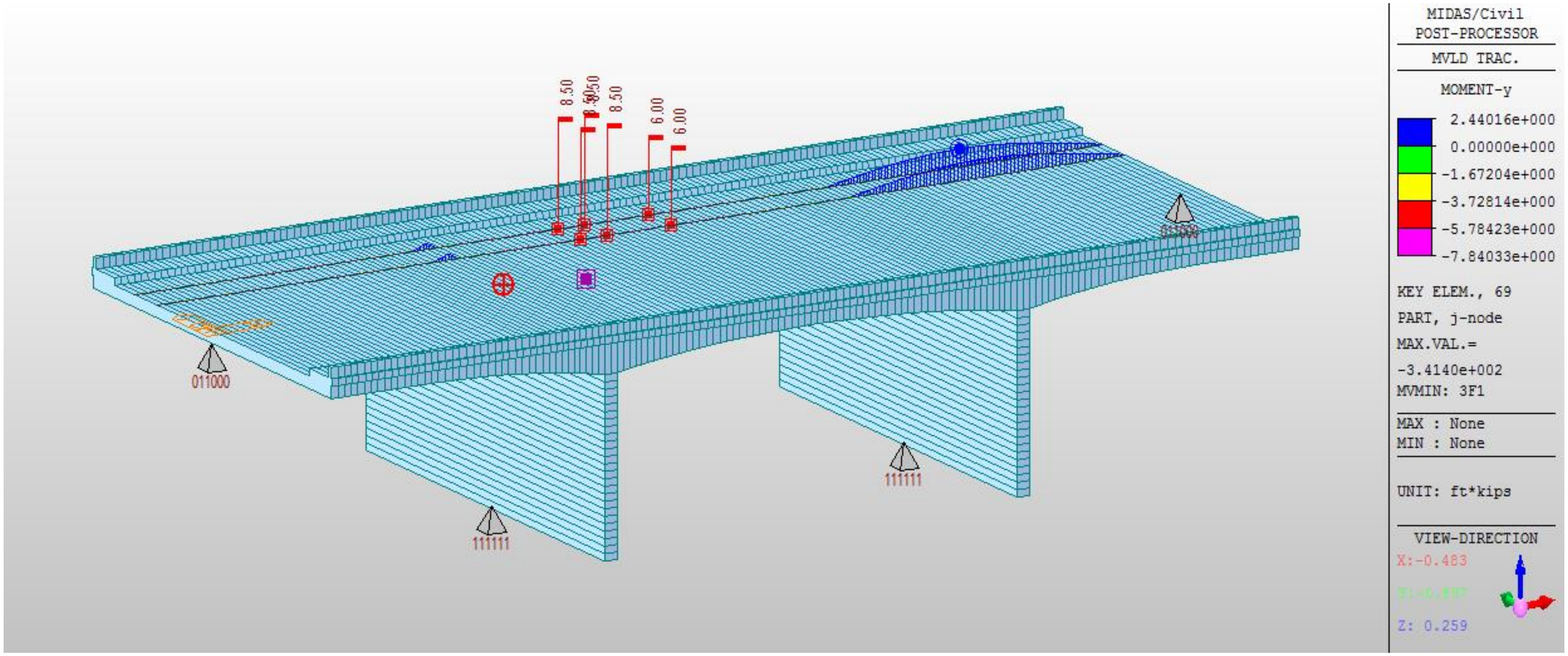


**Figure 2. Critical position of truck and resulting moments as shown in MIDAS/Civil program. Red numbers are load weights in kip (6 kip = 27 kN, 8.5 kip = 38 kN). Moment units listed in the right sidebar are in ft-kip (1 ft-kip = 1.36 m-kN).**

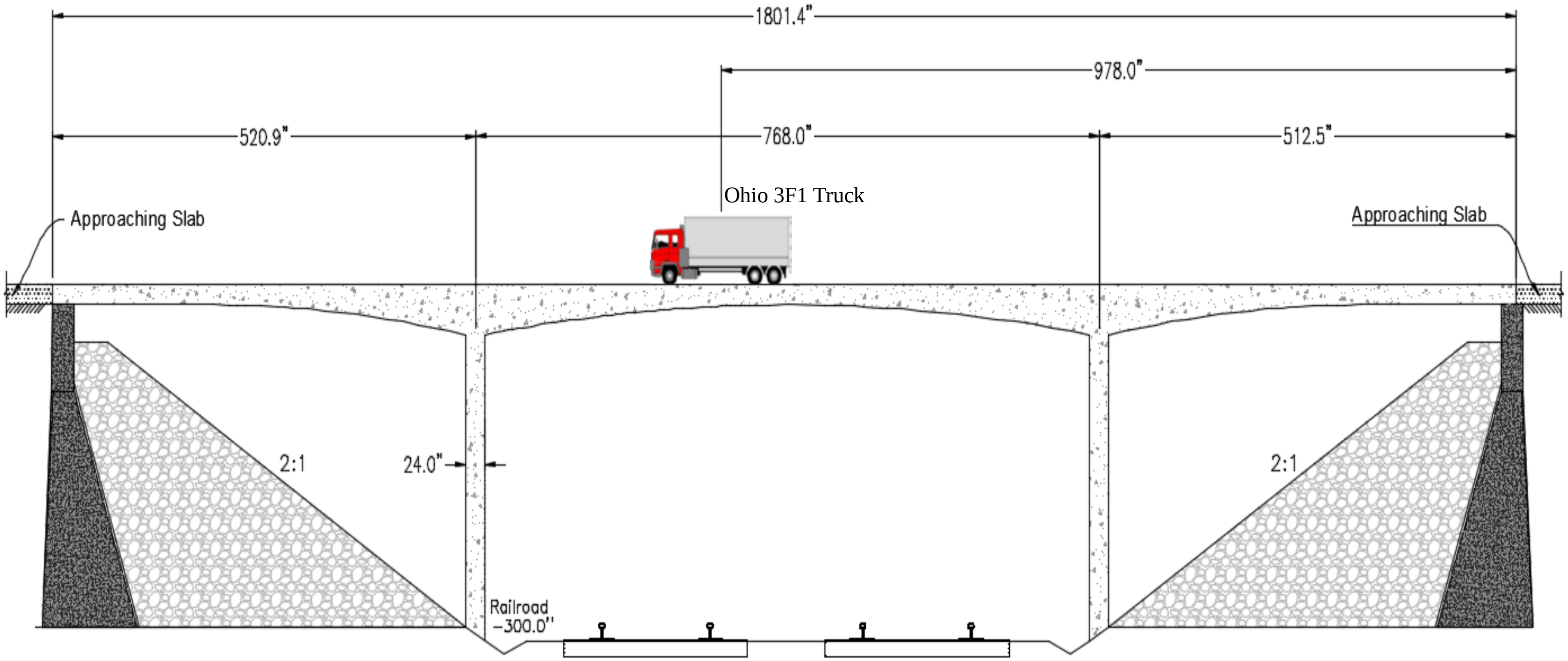


**Figure 3. Bridge LOG-47-1184 profile with load truck in critical position. All dimensions are in inches (39.4 in = 1 m).**

## Instrumentation Plan

Following the initial analysis conducted with MIDAS/Civil, an instrumentation plan was designed for the controlled vehicle load tests on Bridge LOG-47-1184. A field inspection was then undertaken with the assistance of ODOT personnel to help develop a comprehensive instrumentation layout. The field inspection showed that Span 1 was not easily accessible due to obstructions from the adjacent embankments, so Span 3 was selected for instrumentation. Strain gauges were selected for ease of installation and accuracy. In addition, accelerometers were chosen for placement on the bottom of the deck to measure displacement.

Six longitudinally oriented strain gauges were installed in the wheel path and centerline of the driving lane on both the top and bottom surfaces of the slab to provide strain data. Transversely oriented strain gauges were placed at the midpoint between each wheel path and centerline strain gauge. The strain gauges were installed at 5 ft (60 in or 1.5 m) longitudinal intervals from the pier and covered the critical location between 18 ft (216 in or 5.4 m) and 25 ft away (300 in or 7.6 m) from the pier (20.97 ft or 6.39 m for the experimental truck load configuration). Five accelerometers were placed on the bottom of the bridge midway between the longitudinal strain gauges under the center of the lane, except for the two strain gauges nearest the pier. The coordinates for each sensor are given in Appendix 1.

## Controlled Vehicle Load Test Method

### *Instrumentation placement and preparation*

The westbound driving lane of the bridge was closed on May 13, 2019 from the time of the arrival of the snooper truck through completion of the experiment. The ODOT Bridge Inspection Truck (snooper truck) was to be used to assist with sensor installation on the bottom of Span 3. Due to the proximity of the train tracks under Span 2 and trees from the embankment, the ODOT snooper truck could not be used and instead scaffolding was be erected for the installation of strain gauges on the bottom of the slab.

A laser designator was used to locate the wheel path from measurements taken from the edge of the bridge at both ends. From this a grid was created on the bottom of the bridge using markers indicate sensor positions according to the instrumentation plan. Once the process of marking the bridge was completed, the strain gauges and accelerometers were epoxied to the bottom of the bridge and the wires pulled to the outside of the bridge. The sensors and connections attached to the bottom of the bridge are shown in Figure 44.

### *Load test procedure*

The westbound driving lane was closed for testing. The location of the sensors on the top surface was marked using the same reference points used for the bottom of the bridge. The grid system was recreated and the sensor locations marked. The strain gauges were then epoxied to the top of the bridge, and the sensor wires were pulled to the data acquisition system. Figure 55 shows the top bridge deck instrumentation.

Once all the sensors were wired to the data acquisition system, traffic was closed from the entire bridge for approximately 2 minutes to zero the instrumentation. A loaded 3F1 truck with measured wheel loads and equal tire pressures was used for the test; the loads were measured and are shown in Figure6; the total load was 48.15 kip (214.2 kN). The loaded truck was moved into position in the westbound driving lane, which remained closed. When the truck was in position, traffic resumed in the other lanes until it was time to take a measurement. Traffic was cleared from the bridge lanes for approximately two minutes while data were collected. The truck was moved off the bridge and then repositioned in a new location. This process was repeated until data were collected for each truck position. Once the static truck loading was complete, data were collected as the truck passed through the westbound driving lane at speeds of approximately 5 mph (8 km/h), 10 mph (16 km/h), and 15 mph (24 km/h). Traffic was shut down on the entire bridge during each static and moving load test. The static truck positions for each test are presented in Table 1.

**Figure 4. Sensors installed on the bottom of the bridge.**

**Figure 5. Sensors placed on bridge deck.**

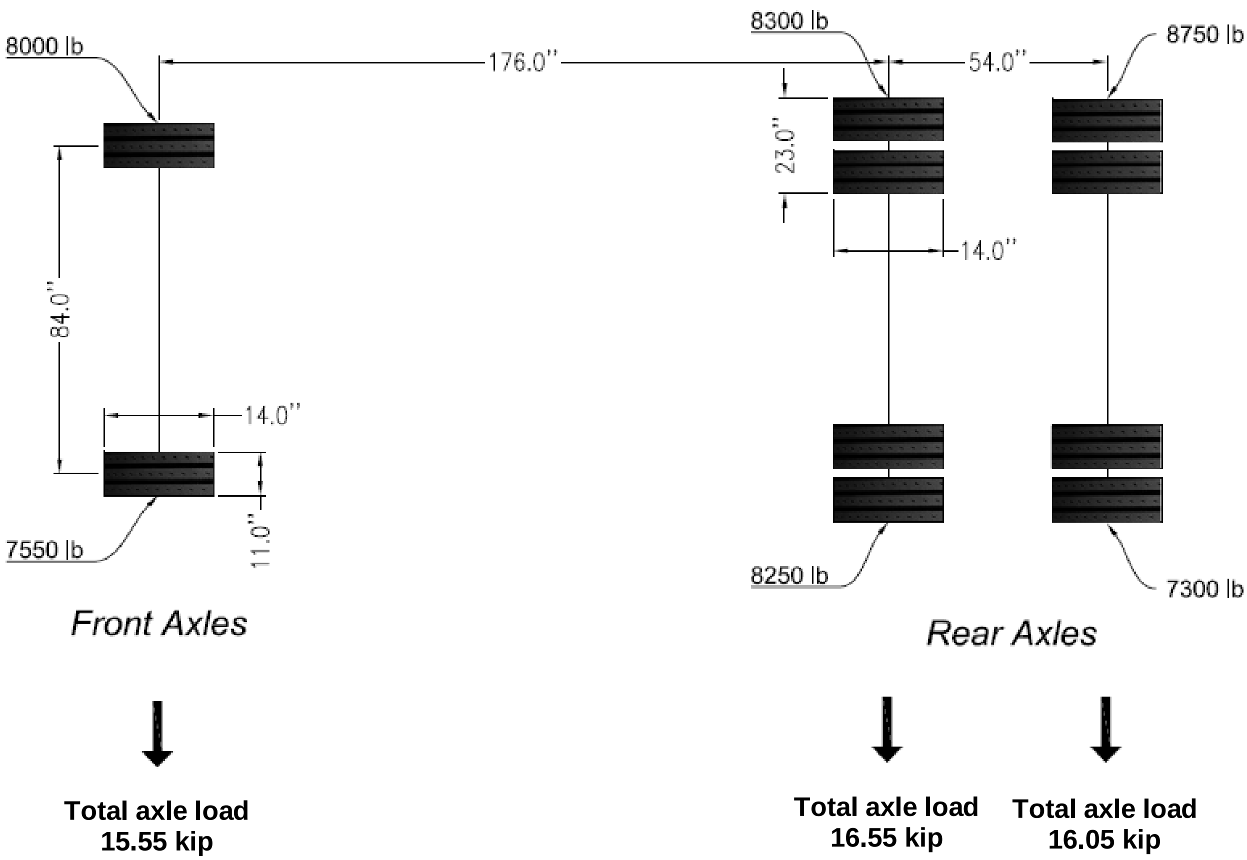


**Figure 6. Diagram showing load and contact points for each wheel of the controlled load truck used in the experiment. (1" = 0.0833 ft = 0.0254 m; 1 lb = 4.45 N; 1 kip = 4.45 kN)**

**Table 1. Static truck load positions. In all cases the truck is oriented longitudinally on the second span.**

| Truck position | Longitudinal distance from abutment | | | Lateral offset from near sidewalk | | | | | |
|---|---|---|---|---|---|---|---|---|---|
| | | | | Front Axle | | Middle Axle | | Rear Axle | |
| | (ft) | (in) | (m) | (in) | (m) | (in) | (m) | (in) | (m) |
| 1A | 51 | 612 | 15.54 | 8 | 0.20 | 14 | 0.36 | 16 | 0.41 |
| 1B | 66.75 | 801 | 20.35 | 9 | 0.23 | 9 | 0.23 | 10 | 0.25 |
| 1C | 82 | 984 | 24.99 | 13 | 0.33 | 8 | 0.20 | 8 | 0.20 |
| 2A | 52 | 624 | 15.85 | 47 | 1.19 | 44 | 1.12 | 44 | 1.12 |
| 2B | 66.75 | 801 | 20.35 | 50 | 1.27 | 46 | 1.17 | 45 | 1.14 |
| 2C | 82.17 | 986 | 25.05 | 51 | 1.30 | 48 | 1.22 | 48 | 1.22 |

# Results

## *Experimental determination of RFs*

The strains measured in the controlled vehicle load tests were used to determine the moment at the location of the gauges assuming a 1 ft (12 in or 0.305 m) wide section. These moments were then multiplied by a strip width $W_s$ of 6.52 ft (75 in or 1.9 m) determined from the equation in AASHTO Standard Specifications Article 3.24.3.2 ($W_s = 4 + 0.06*S$). The dynamic load allowance factor (IM) of 1.33 was then applied to the moment. Experimentally determined operating Rating Factors (RFs) are shown in Table 2.

**Table 2. Operating Rating Factors (RFs) for experimental truck positions.**

| Test | Longitudinal position of load relative to Pier 2 | | | Operating RF | | RF Ratio |
|---|---|---|---|---|---|---|
| | (in) | (ft) | (m) | Experimental | MIDAS/Civil | |
| 1B | 240 | 20 | 6.10 | 1.865 | 1.764 | 0.946 |
| | 300 | 25 | 7.62 | 5.345 | 2.991 | 0.560 |
| | 360 | 30 | 9.14 | 5.442 | 4.535 | 0.833 |
| 1C | 240 | 20 | 6.10 | 2.428 | 1.267 | 0.522 |
| | 300 | 25 | 7.62 | 4.474 | 2.148 | 0.480 |
| | 360 | 30 | 9.14 | 7.295 | 3.256 | 0.446 |
| 2B | 240 | 20 | 6.10 | 2.137 | 1.764 | 0.825 |
| | 300 | 25 | 7.62 | 8.515 | 2.991 | 0.351 |
| | 360 | 30 | 9.14 | 6.558 | 4.535 | 0.692 |
| 2C | 240 | 20 | 6.10 | 2.165 | 1.260 | 0.582 |
| | 300 | 25 | 7.62 | 8.345 | 2.136 | 0.256 |
| | 360 | 30 | 9.14 | 6.927 | 3.238 | 0.467 |

## *Analytical determination of RFs using MIDAS/Civil*

Since the experimental testing consisted of only a single truck in multiple locations, several MIDAS/Civil models were created with load matching that of the truck used for experimental testing. The MIDAS/Civil models consisted of a 1 ft (12 in or 0.305 m) strip width of the bridge (unit width model), a full width model of the bridge excluding sidewalks and parapets, and a full width model including sidewalks and parapets. The models were then loaded with the truck used in experimental testing and the typical load rating truck configurations. The moments determined from the MIDAS/Civil models for the standard trucks are provided in Table 3 at the critical location determined from the original ODOT BrR analyses. The moments for the full width without the sidewalks and parapets are slightly lower than the unit width model. This is likely due to the distribution of the moment over the width. However, the moments for the model with the sidewalks and parapets are higher than the unit width model. This is likely due to the truck position in the driving lane where the higher stiffness from the sidewalks and parapets has an effect. The moments from the unit width model were used since the parapets and sidewalks were not considered in the analyses performed by ODOT. The moments were then multiplied by the distribution factor of 0.1534 determined from AASHTO as $1/(4 + 0.06*S)$ and dynamic load allowance factor (IM) of 1.33.

The Rating Factors (RFs) were determined using the Load Factor Rating equation for the operating condition using the load factors of 1.3 for A1 and A2. RFs from the experimental testing and from the MIDAS model are provided in Table 3 along with the ratio of RFs.

**Table 3. MIDAS/Civil moments at critical location 20.97 ft (251.6 in = 6.39 m from Pier 2).**

| Truck configuration | Unit width moment (1 ft = 0.305 m) | | Full width of all traffic lanes (52 ft = 624 in = 15.85 m) | | Full Width (parapet-to-parapet) (64 ft = 768 in = 19.51 m) | |
|---|---|---|---|---|---|---|
| | (kip-ft) | (m-kN) | (kip-ft) | (m-kN) | (kip-ft) | (m-kN) |
| EV2 | -113.48 | -153.86 | -108.64 | -147.30 | -133.27 | -180.69 |
| EV3 | -169.11 | -229.28 | -161.88 | -219.48 | -198.58 | -269.24 |
| HS 20-44 | -134.42 | -182.25 | -128.64 | -174.41 | -158.61 | -215.05 |
| OH-2F1 | -64.06 | -86.85 | -61.56 | -83.46 | -74.36 | -100.82 |
| OH-3F1 | -96.39 | -130.69 | -94.98 | -128.78 | -112.19 | -152.11 |
| OH-4F1 | -110.42 | -149.71 | -105.72 | -143.34 | -128.91 | -174.78 |
| OH-5C1 | -96.02 | -130.19 | -91.86 | -124.55 | -113.08 | -153.32 |
| SU4 | -109.91 | -149.02 | -105.22 | -142.66 | -128.39 | -174.07 |
| SU5 | -122.05 | -165.48 | -116.83 | -158.40 | -143.19 | -194.14 |
| SU6 | -135.44 | -183.63 | -129.68 | -175.82 | -159.04 | -215.63 |
| SU7 | -147.49 | -199.97 | -141.22 | -191.47 | -173.49 | -235.22 |

### *Analytical determination of RFs using ABAQUS*

A full width model that included sidewalks and parapets was created in ABAQUS. The model was calibrated with the experimental results and then used to assess the load rating for the other truck configurations. Moments were found from output strains of the models loaded with the standard rating trucks in the same manner as was done for the experimental results. The Rating Factors (RFs) were determined using the Load Factor Rating equation for the operating condition using the load factors of 1.3 for A1 and A2. Operating RFs from the original BrR, MIDAS, and ABAQUS models are provided in Table 4 along with ratios of the RFs for BrB to MIDAS and BrB to ABAQUS. The MIDAS model still showed posting would be required based on the EV3 vehicle while the ABACUS model showed no posting would be necessary. The RF ratios for the BrR and MIDAS models was approximately 0.6. The ratios of the BrR to ABAQUS RFs was approximately 0.3 with the exception for the 2F1 truck loading which was 0.4.

The original RFs determined using the unsupported PC BARS program were not supplied to the research team, and thus could not be compared with any of the computed RFs.

It should be noted that the NCHRP Project 20-07 / Task 410 report [HNTB and Ghosn, 2019] implies that the live load factors for EV2 and EV3 should be different in order to achieve average reliabilities close to the LRFR target reliability index of 2.50. Using a $\gamma_{LL}$= 1.40 for EV2 achieved an average reliability index equal to 2.47, close to the 2.50 target. Using a $\gamma_{LL}$= 1.10 for EV3 resulted in an average reliability index of 2.41 while a $\gamma_{LL}$= 1.30 resulted in an average reliability index of 2.78. Table 5 provides the operating RFs for EV2 and EV3 using $\gamma_{LL}$= 1.40 and $\gamma_{LL}$= 1.10, respectively.

**Table 4. Operating RFs and ratios for standard truck configurations.**

| Truck | RF | | | Ratio | |
|---|---|---|---|---|---|
| | BrR | MIDAS | ABAQUS | BrR / MIDAS | BrR / ABAQUS |
| EV2 | 0.698 | 1.180 | 2.178 | 0.592 | 0.321 |
| EV3 | 0.467 | 0.792 | 1.464 | 0.590 | 0.319 |
| HS 20-44 | 0.580 | 0.996 | 1.813 | 0.582 | 0.320 |
| OH-2F1 | 1.264 | 2.089 | 3.110 | 0.605 | 0.406 |
| OH-3F1 | 0.834 | 1.389 | 2.719 | 0.601 | 0.307 |
| OH-4F1 | 0.725 | 1.212 | 2.371 | 0.598 | 0.306 |
| OH-5C1 | 0.817 | 1.394 | 2.672 | 0.586 | 0.306 |
| SU4 | 0.727 | 1.218 | 2.380 | 0.597 | 0.306 |
| SU5 | 0.649 | 1.097 | 2.131 | 0.592 | 0.305 |
| SU6 | 0.584 | 0.988 | 1.919 | 0.591 | 0.304 |
| SU7 | 0.535 | 0.908 | 1.756 | 0.590 | 0.305 |

**Table 5. Operating RFs for revised load factors.**

| Truck | $\gamma_{LL}$ | Reliability Index | RF | |
|---|---|---|---|---|
| | | | MIDAS | ABAQUS |
| EV2 | 1.40 | 2.47 | 1.095 | 2.022 |
| EV3 | 1.10 | 2.41 | 0.935 | 1.730 |

## Conclusions and Recommendations

Based on the study the following conclusions can be made.

- Using the MIDAS/Civil model resulted in more accurate moments and higher RFs than the BrB model by a factor of about 1.67.
- Using the typical live load factor of $\gamma_{LL}$= 1.30 resulted in all trucks having RFs greater than 0.9 with the exception of EV3. However, using $\gamma_{LL}$= 1.10 based on the NCHRP 20-07/Task 410 report [HNTB and Ghosn, 2019] for EV3 resulted in a RF of 0.935. Using a $\gamma_{LL}$= 1.40 based on the NCHRP 20-07/Task 410 report for EV2 resulted in a RF of 1.095.
- Using the ABAQUS model calibrated from experimental field loading of the bridge, resulted in more accurate moments and higher RFs than the BrB and MIDAS/Civil models.
- The ABACUS model increased the RFs determined by the BrR model by a factor of approximately 3.3 for all rating trucks with the exception of the 2F1 truck loading which was 2.5.
- The ABAQUS model resulted in RFs all above 1.0 with the controlling RF being 1.464 for EV3 when using the typical live load factor of $\gamma_{LL}$= 1.30. Using a $\gamma_{LL}$= 1.10 based on NCHRP 20-07/Task 410 for EV3 resulted in a RF of 1.730.

The MIDAS/Civil and ABAQUS models for LOG 47-1184 resulted in RFs higher than provided by the BrB model. Though the increases were fairly constant for each model, this was for only one specific slab arch bridge. Additional similar analyses of other concrete slab bridges would provide a more comprehensive and consistent picture of the average increase from using these models.

## References

American Association of State Highway and Transportation Officials (AASHTO). (2018). *The Manual for Bridge Evaluation*, 3rd Edition, Washington, D.C

American Association of State Highway and Transportation Officials (AASHTO). (2017). *LRFD Bridge Design Specifications*, 8th Edition, Washington, DC.

American Association of State Highway and Transportation Officials (AASHTO). (2002). *Standard Specifications for Highway Bridges*, 17th Edition, Washington, DC.

American Association of State Highway and Transportation Officials (AASHTO). (1994), *Manual for Condition Evaluation of Bridges*, 2nd Ed., Washington, D.C.

American Association of State Highway and Transportation Officials (AASHTO), 1992. *Standard Specifications for Highway Bridges*, 15th Edition, Washington, DC.

Davids, W. G., Poulin, T. J., & Goslin, K. (2013). "Finite-element analysis and load rating of flat slab concrete bridges". *Journal of Bridge Engineering*, *18*(10), 946-956.

HNTB Corporation and Ghosn, Michael. (2019, March). *Load Rating for the Fast Act Emergency Vehicles Ev-2 and Ev-3*. Revised Final Report for the National Cooperative Highway Research Program of the Transportation Research Board, National Research Council. NCHRP Project 20-07/Task 410. Available online at http://onlinepubs.trb.org/onlinepubs/nchrp/docs/NCHRP20-07Task410FinalReport_March2019.pdf, accessed September 16, 2019.

Miller, R. A., Aktan, A. E., & Shahrooz, B. M. (1992, April). "Nondestructive and destructive testing of a three span skewed RC slab bridge". *Nondestructive testing of concrete elements and structures* (pp. 150-161). ASCE.

Saraf, V. K. (1998). "Evaluation of existing RC slab bridges". *Journal of Performance of Constructed Facilities*, *12*(1), 20-24.

**Appendix 1: Coordinate positions of sensors on Bridge LOG-47-1184**

In this experiment, the x coordinate is measured to the left from the right abutment, the y coordinate is measured down from where the sidewalk meets the driving lane along the abutment, and the z axis is measured into the page from the driving surface. Because the y coordinate is measured along the abutment, the y axis is not perpendicular to the x axis, but is skewed by 14°29′. The sensors attached at the bottom of the bridge have a negative z coordinate because they are below the driving surface.

| Sensor ID | Offset from Pier 2 (ft) | (in) | (m) | Longitudinal distance from abutment (x) (ft) | (in) | (m) | Skew lateral offset from near sidewalk (y) (in) | (m) | Thickness, or distance below surface (z) (in) | (m) |
|---|---|---|---|---|---|---|---|---|---|---|
| BL1 | 5 | 60 | 1.52 | 111.7 | 1341 | 34.05 | 54 | 1.37 | -41.4 | -1.05 |
| BL2 | 10 | 120 | 3.05 | 116.7 | 1401 | 35.57 | 54 | 1.37 | -32.9 | -0.84 |
| BL3 | 15 | 180 | 4.57 | 121.7 | 1461 | 37.10 | 54 | 1.37 | -26.6 | -0.68 |
| BL4 | 20 | 240 | 6.10 | 126.7 | 1521 | 38.62 | 54 | 1.37 | -22.6 | -0.57 |
| MM | 20.97 | 251.64 | 6.39 | 127.7 | 1532 | 38.92 | 54 | 1.37 | -22.0 | -0.56 |
| BL5 | 25 | 300 | 7.62 | 131.7 | 1581 | 40.14 | 54 | 1.37 | -20.7 | -0.53 |
| BL6 | 30 | 360 | 9.14 | 136.7 | 1641 | 41.67 | 54 | 1.37 | -20.5 | -0.52 |
| BT1 | 5 | 60 | 1.52 | 111.7 | 1341 | 34.05 | 76 | 1.93 | -41.4 | -1.05 |
| BT2 | 10 | 120 | 3.05 | 116.7 | 1401 | 35.57 | 76 | 1.93 | -32.9 | -0.84 |
| BT3 | 15 | 180 | 4.57 | 121.7 | 1461 | 37.10 | 76 | 1.93 | -26.6 | -0.68 |
| BT4 | 20 | 240 | 6.10 | 126.7 | 1521 | 38.62 | 76 | 1.93 | -22.6 | -0.57 |
| MM | 20.97 | 251.64 | 6.39 | 127.7 | 1532 | 38.92 | 76 | 1.93 | -22.0 | -0.56 |
| BT5 | 25 | 300 | 7.62 | 131.7 | 1581 | 40.14 | 76 | 1.93 | -20.7 | -0.53 |
| BT6 | 30 | 360 | 9.14 | 136.7 | 1641 | 41.67 | 76 | 1.93 | -20.5 | -0.52 |
| BL12 | 5 | 60 | 1.52 | 111.7 | 1341 | 34.05 | 96 | 2.44 | -41.4 | -1.05 |
| BL11 | 10 | 120 | 3.05 | 116.7 | 1401 | 35.57 | 96 | 2.44 | -32.9 | -0.84 |
| AC1 | 12.5 | 150 | 3.81 | 119.2 | 1431 | 36.33 | 96 | 2.44 | -29.5 | -0.76 |
| BL10 | 15 | 180 | 4.57 | 121.7 | 1461 | 37.10 | 96 | 2.44 | -26.6 | -0.68 |
| AC2 | 17.5 | 210 | 5.33 | 124.2 | 1491 | 37.86 | 96 | 2.44 | -24.3 | -0.62 |
| BL9 | 20 | 240 | 6.10 | 126.7 | 1521 | 38.62 | 96 | 2.44 | -22.6 | -0.57 |
| MM | 20.97 | 251.64 | 6.39 | 127.7 | 1532 | 38.92 | 96 | 2.44 | -22.0 | -0.56 |
| AC3 | 22.5 | 270 | 6.86 | 129.2 | 1551 | 39.38 | 96 | 2.44 | -21.3 | -0.54 |
| BL8 | 25 | 300 | 7.62 | 131.7 | 1581 | 40.14 | 96 | 2.44 | -20.7 | -0.53 |
| AC4 | 27.5 | 330 | 8.38 | 134.2 | 1611 | 40.91 | 96 | 2.44 | -20.6 | -0.52 |
| BL7 | 30 | 360 | 9.14 | 136.7 | 1641 | 41.67 | 96 | 2.44 | -20.5 | -0.52 |
| AC5 | 32.5 | 390 | 9.91 | 139.2 | 1671 | 42.43 | 96 | 2.44 | -20.5 | -0.52 |

Sensor ID Key: AC = Accelerometer, BL = Bottom Longitudinal strain gauge, BT = Bottom Transverse strain gauge, TL = Top Longitudinal strain gauge, TT = Top Transverse strain gauge, MM = Maximum Moment critical location determined by MIDAS/Civil.